Hydrophilicity of Graphene in Water through Transparency to Polar and Dispersive Interactions

Belyaeva, L.; Deursen, P.M.G. van; Barbetsea, K.I.; Schneider, G.F.

ADVANCED MATERIALS
www.advmat.de

Hydrophilicity of Graphene in Water through Transparency to Polar and Dispersive Interactions

*Liubov A. Belyaeva, Pauline M. G. van Deursen, Kassandra I. Barbetsea, and Grégory F. Schneider**

Establishing contact angles on graphene-on-water has been a long-standing challenge as droplet deposition causes free-floating graphene to rupture. The current work presents ice and hydrogels as substrates mimicking water while offering a stable support for graphene. The lowest water contact angles on graphene ever measured, namely on graphene-on-ice and graphene-on-hydrogel, are recorded. The contact angle measurements of liquids with a range of polarities allow the transparency of graphene toward polar and dispersive interactions to be quantified demonstrating that graphene in water is hydrophilic. These findings are anticipated to shed light on the inconsistencies reported so far on the wetting properties of graphene, and most particularly on their implications toward rationalizing how molecules interact with graphene in water.

The wetting properties of graphene are more complicated than those found in regular solid–liquid interfaces. Free-standing graphene possesses no bulk phase and is only composed of a single atomic layer of carbon atoms separating two liquid media. Graphene is therefore subjected to a variety of non-specific interactions with adsorbates at the graphene–liquid interfaces.[1]

Wetting transparency, opacity, hydrophilicity, and hydrophobicity of graphene remain under debate. Intensive recent studies report evidence for the wetting transparency of graphene, suggesting that the wettability of graphene is governed by the wettability of the underlying support.[1–3] Other studies report complete wetting transparency of graphene when deposited on gold, copper, and silicon, but not glass, where interactions with water are considered short-range.[2] A later experimental work supported by molecular dynamics simulations suggests partial transparency of graphene and indicates that wetting transparency does not occur for superhydrophilic or superhydrophobic substrates,[3] and a number of papers suggests full wetting opacity of monolayer graphene irrespective of the substrate with contact angle values similar to water contact angle on graphite.[4–6] Consequently, contact angle values of water on graphene vary from 33° for graphene on silicon[2] to 90°–127° for graphene respectively on silicon carbide, silicon oxide, and copper[4–7] despite a large number of theoretical studies suggesting that water contact angle values on graphene should be similar to the one of graphite.[1,4,6] So far, contradictions and inconsistencies have partially been suggested to be caused by the presence of adsorbates, graphene defects, and surface charges.[8,9]

Concerning the wetting properties of graphene in water, the direct measurement of the contact angle of water on graphene-on-water—i.e., depositing a droplet of water on graphene floating on water—has been technically impossible due to the immediate rupture of graphene upon droplet deposition (**Figure 1**a,b) resulting from growth- and handling-induced cracks and tears.[10–13] Probing wetting properties of graphene in water and water solutions is, however, particularly important for application in sensing, water filtration, fuel cell membranes, and more generally when graphene is exposed to water from the both sides.[1,14–16] Here, we show that graphene is surprisingly hydrophilic when floating on water. Additionally, by changing the polarity of the liquid used to measure contact angles (both of the drop and of the solution), we calculated the surface energy of graphene showing that monolayer graphene is transparent to both polar and dispersive interactions—i.e., fully transparent to wetting—with the condition that the substrate/graphene/liquid interface is smooth and free of contaminations. In the contrary case—that is when graphene is physically transferred from the growth substrate to another support—graphene usually does not conform perfectly the target substrate resulting in the screening of short-range polar interactions while long-range dispersion interactions are fully transmitted. The latter often occurs when graphene is transferred with the use of a polymer yielding surface corrugations, wrinkles, contamination, large sample-to-sample variations, and immense discrepancies in contact angle measurements.

To quantify and rationalize the hydrophobicity of graphene in wet environment, we introduce ice and hydrogels as models of liquid water. In fact, the water molecules at the surface of ice are in a supercooled liquid state retaining an amorphous liquid-like structure.[17–21] This makes the surface of ice an

L. A. Belyaeva, P. M. G. van Deursen, K. I. Barbetsea, Dr. G. F. Schneider
Faculty of Science
Leiden Institute of Chemistry
Leiden University
Einsteinweg 55, 2333CC Leiden, The Netherlands
E-mail: g.f.schneider@chem.leidenuniv.nl

DOI: 10.1002/adma.201703274

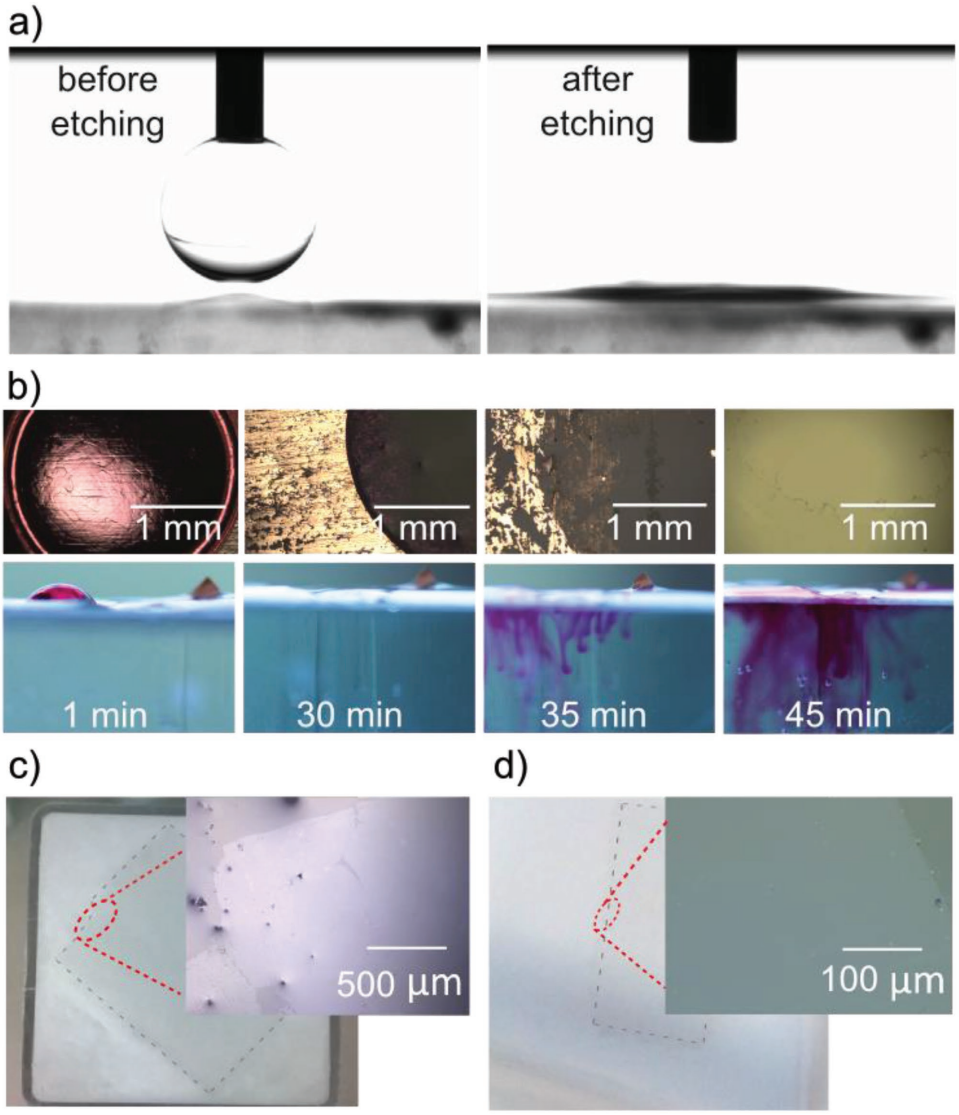

Figure 1. Graphene free-floating on liquid water, ice, and hydrogels. a) Water contact angle (WCA) measurements of graphene floating on a water surface. Left: water droplet before being deposited on the surface of chemical vapor deposition (CVD)-graphene floating on an aqueous solution of copper etchant. Right: a water droplet after being deposited on the surface of graphene sinks through the graphene, preventing the measurement of the contact angle. The rupture and consequent breaking of the graphene is also seen in the case of pure water instead of APS solution. b) Time lapse photographs of a water droplet sinking through a graphene/copper stack floating on the surface of an aqueous solution of ammonium persulfate (copper etchant) as a function of copper etching time (from left to right). Photographs were taken from the top of the droplet (top images) and from the side (bottom images). The water droplet was dyed with Rhodamine B for optimal visualization. c) Photograph and optical microscopy image (inset) of a monolayer of graphene on ice. d) Photograph and optical microscopy image (inset) of a monolayer of graphene on a 4% agarose hydrogel.

eligible aproximation of the surface of water. As for hydrogel a low weight percent agarose has a low surface concentration of polymer chains relative to that of interstitial water and, for that reason, has been used as a quasisolid model for water surface properties since the 1960s.[22,23] By experimentally measuring the contact angle of graphene on water, we observed the lowest contact angle reported for graphene so far: 30° ± 5° on ice and 10° ± 2° on a 4 wt% agarose hydrogel.

Importantly, the cleanliness of the graphene surface and of the graphene–substrate interface are critical factors for reliable contact angle measurements. Great care must be taken to avoid or minimize contamination by e.g. polymer residues and hydrocarbon adsorbates. For details on our cleaning (e.g., from polymer residuals or hydrocarbon adsorbates), handling, and control measurements protocols, we refer the reader to the Supporting Information.

To illustrate the nessecity of a solid-like support for contact angle measurements, we shall shortly consider graphene on liquid water (Figure 1). Intact graphene floats on water—presenting a graphene-on-water surface—but the contact angle of its surface cannot be measured because free-floating graphene immediately breaks apart when a droplet of water is casted onto the graphene top surface, inducing excessive mechanical and interfacial stress resulting in cracking and

tearing of graphene (Figure 1a). Those microcracks might result from the growth,[10,11,13] appear during copper etching[10–12] or simply under the droplet pressure. The water droplet therefore sinks through graphene even if the droplet is deposited before copper is completely etched away, i.e., when the dynamic stress in graphene is minimized (Figure 1b).

To overcome this limitation and to probe the wetting properties of graphene in water we replaced liquid water underneath graphene with water ice and hydrogels (Figure 1c,d). These systems are especially benign to graphene as they avoid using a protective polymer (usually poly(methyl methacrylate) (PMMA)) layer that always yields contamination such as polymer left-overs.

In the ice system, graphene grown by chemical vapor deposition (CVD) on copper (see Methods in the Supporting Information for details) is placed on the surface of an aqueous solution of 0.5 M ammonium persulfate (APS), which etches copper. After cool-down and the solidification of water, the contact angle of a droplet of water deposited on graphene-on-ice was measured. To prevent water condensation, the chamber was flushed with dry air during the process of water freezing and measurement. Another possible source of inaccuracy in measurements is strain in graphene that may be induced upon freezing of water. However, we will show later that it does not affect the wetting transparency, as in the case of strain no significant change in graphene-ice distance occurs to screen the interactions since the contact angle and surface energy of graphene on ice are very close to those of bare ice.

Remarkably, the water contact angle (WCA) on graphene-on-ice at 0 °C is 30° ± 5° which is only 13° greater than the water contact angle of pure ice and 30° smaller than the water contact angle of freshly exfoliated graphite (see **Figure 2**a). Repeating the experiment with double layer graphene increases the WCA to 35° on average. At −20 °C the WCA also showed similar hydrophilic behavior of graphene when deposited on ice (see Figure 2a). To prevent the water droplet from instant freezing at the moment of its deposition on graphene we added 18% of nitric acid (see Methods in the Supporting Information). This addition yields slightly smaller contact angles compared to experiments carried at 0 °C due to the increase in the polarity of the liquid droplet: 11° ± 3° for ice, 18° ± 4° for monolayer graphene on ice, 34° ± 5° for bilayer graphene on ice, and 57° ± 2° for graphite. The effect of added nitric acid on the contact angle and on the surface energy was accounted by the approach typically used for an electrolyte solution (experimental details and calculations of the surface energy can be found in the Supporting Information). One and two layers of graphene, therefore, transmit a major portion of water–water interactions, although the bilayer is less hydrophilic and screens a noticeable part of the interactions due to the increased thickness.

Interestingly, graphene suspended on a hydrogel provides results very similar to graphene on ice. In the graphene-hydrogel system developed for contact angle measurements, CVD graphene grown on copper is supported by a 4% agarose gel network while APS solution contained in the gel etches the copper.[24]

Graphene on hydrogel is hydrophilic, with a contact angle of 10° ± 2° for single layer graphene. Optical microscopy images of graphene on hydrogel after contact angle measurement with water (left) and diiodomethane (right) are shown in Figure 2b. The microscopy images show that multiple cracks have formed after the deposition of a water droplet (Figure 2b, left) while an intact surface is preserved during the deposition of organic liquids (Figure 2b, right). The cracking under the influence of water is attributed to the strong interactions between water underneath graphene and water in the droplet. Despite the appearance of cracks, no water leaks away into the gel, as water droplets attain a stable shape three seconds after the deposition of the droplet—during which the droplet spreads out. Moreover, graphene coverage, despite cracks, was still well above 95%, with no noticeable cracks on the periphery of the droplet. It's worth noting that analogous crack analysis was not possible for ice samples due to technical limitations: the sample has to be cooled down so the liquid droplet does not evaporate after the contact angle measurement. Therefore we could not inspect the surface of graphene on ice with a microscope after the contact angle measurement.

By measuring contact angles of water-immiscible solvents on hydrogels with a range of agarose concentrations, a linear extrapolation was made to 100% water.[22] Figure 2c shows the linear extrapolation of the contact angle of diiodomethane on hydrogel composed of 1–4% agarose (see Figure S1 in the Supporting Information for the extrapolation with 1-methylnaphtalene). From the extrapolation, the contact angle of diiodomethane on water would be 41°. Conversely, such data cannot be gathered for graphene-on-hydrogel, because graphene relies on a high (4%) agarose concentration for mechanical support.

In summary, two independent experiments have proven that when placed in a water-like environment, graphene, surprisingly, presents hydrophilic properties very close to those of pure water. In other words, graphene is transparent to water–water interactions. Studying only graphene–water interactions, however, is not sufficient for understanding graphene wetting properties and claiming its wetting transparency.

For that reason we also conducted contact angle measurements with other liquids possessing different polarities (Table S1 in Methods of the Supporting Information). With all probed liquids graphene deposited on ice and hydrogel showed a contact angle similar to the contact angles on pure ice (Figure 2d,e). Contact angles with organic liquids seem to be more reliable than those with water, as no damage to the graphene structure occurs during the measurement (see Figure 2b for comparison).

To explain the inconsistencies in literature on the water contact angle of graphene, we first questioned whether the great variety of WCA reported for graphene suggests that graphene transmits only a part of the interactions. In that case, transparency or opacity of graphene to wetting is determined by the dominating type of interactions between the droplet molecules and the substrate and its transmission through a graphene layer. Depending on the chemical nature of the adsorbate and adsorbent, all intermolecular interactions can be divided into two main groups: site-specific polar (hydrogen bonding, dipole–dipole, and dipole-induced interactions) and nonspecific dispersive interactions (London–van der Waals interactions).[25,26] Polar interactions appear whenever the electron density or a positive charge is localized along the bonds. Dispersive interactions appear due to instantaneous dipole

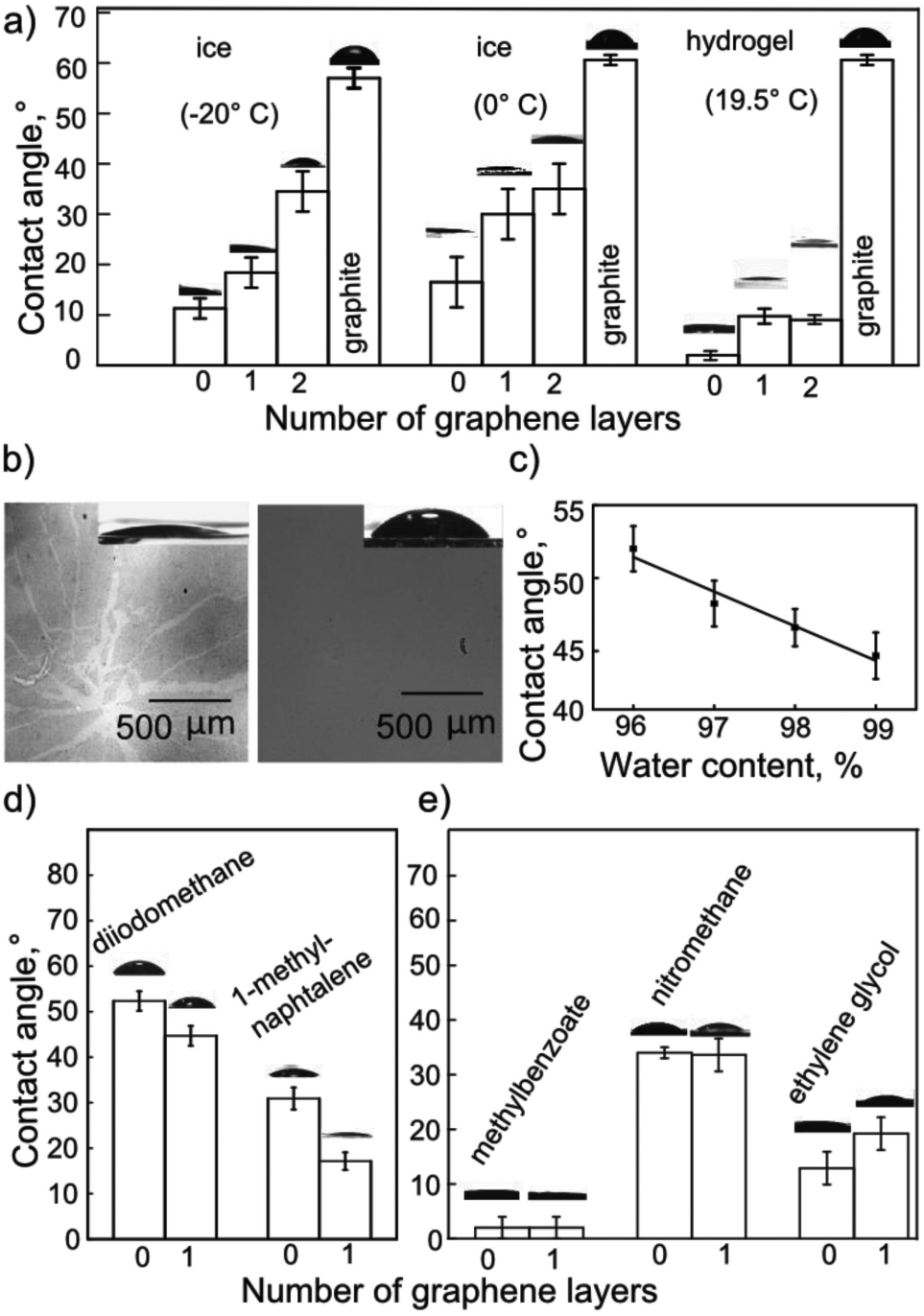

Figure 2. Contact angles of graphene on ice and hydrogel. a) WCA of graphene on ice measured at –20 °C, 0 °C, and for graphene on a 4% agarose hydrogel measured at 19.5 °C. WCA were measured for bare ice/hydrogel, monolayer graphene, and bilayer graphene. b) Contact angle photographs (insets) and optical microscopy images of the graphene after dropcasting water (left) and diiodomethane (right) on top of graphene floating on a 4% agarose hydrogel. The process of dropcasting a droplet of water typically causes graphene cracking while dropcasting of an organic liquid leaves no visible damages on graphene. c) Hydrogel as a water model: diiodomethane contact angles for an agarose hydrogel with different water content. d) Contact angles of graphene on a 4% agarose hydrogel with diiodomethane and 1-methylnaphtalene as liquid droplets. e) Contact angles of graphene on ice with methylbenzoate, nitromethane, and ethylene glycol.

moments of all atoms and molecules and, therefore, always present themselves regardless of chemical nature of the interacting molecules. These two types of interactions can be quantified in terms of surface energy components.[26,27] According to the Owens and Wendt[26] or Fowkes[22] theory the total surface tension of a liquid or a solid can be represented as a sum of polar and dispersive components corresponding to polar and dispersive interactions

$$\sigma_L = \sigma_L^P + \sigma_L^D \quad (1)$$

$$\sigma_S = \sigma_S^P + \sigma_S^D \quad (2)$$

and all four components can be related according to the Owens–Wendt equation

$$\frac{\sigma_L(\cos\theta + 1)}{2\sqrt{\sigma_L^D}} = \frac{\sqrt{\sigma_S^P}\sqrt{\sigma_L^P}}{\sqrt{\sigma_L^D}} + \sqrt{\sigma_S^D} \quad (3)$$

We also calculated the surface energies by the Fowkes model[22,27] and found them in good agreement with those calculated according to the Owens–Wendt model (see Figure S2 in the Supporting Information). Detailed calculations of surface energies using the Owens–Wendt theory and results of the Fowkes calculations can be found in the Supporting Information.

Probing contact angles of liquids with different polarities allows the determination of the polar σ_S^P and dispersive σ_S^D components of the solid and identifies the character of the interactions between the droplet and the solid.[26] We examined the variation of σ_S^P and σ_S^D caused by the addition of a graphene layer in order to determine what interactions are transmitted or screened by the graphene and to what extent. Water, diiodomethane, and 1-methylnaphthalene were chosen because of their compatibility with the hydrogel matrix. Their polar and dispersive components are tabulated (see Table S1 in Methods of the Supporting Information). Water, methyl benzoate, nitromethane, and ethylene glycol were chosen as test liquids for ice due to their low freezing points and known polar and dispersive components; and water, diiodomethane, formamide, nitromethane, and methyl benzoate were chosen for SiO_2/Si, polydimethylsiloxane (PDMS), and copper (Table S1 in Methods of the Supporting Information).

In addition to ice and water, which are predominantly polar, two complementary types of substrates were selected, namely substrates with similar polar and dispersive components (i.e., SiO_2/Si wafers and PDMS), and a substrate with a dominating dispersive component (i.e., copper). Importantly, because graphene has not been transferred on copper, ice, and hydrogel (see Methods in the Supporting Information for the details on the samples preparation), it conforms to the surfaces allowing for a perfect adhesion.[28] On the contrary, graphene being transferred from copper onto another solid substrate cannot conform as effectively to the surface and possesses multiple out-of-plane irregularities such as wrinkles, buckling's, foldings, and so on,[29,30] resulting in larger graphene–substrate separation and, consequently, poorer adhesion.[28]

As shown in Figure 2, graphene does not alter contact angles of all tested liquids when deposited on top of copper, ice, or hydrogel, and, consequently, transmits both polar and dispersive interactions (**Figure 3**). We must note here that an increase in the number of graphene layers results in poorer reproducibility due to contamination, defect formation, and uncontrollable interlayer distance occurring during the transfer of the layers on top of each other (we purchased the multilayer samples from Graphenea, which is prepared by the "repeat transfer" method). The error margins are therefore wider for bilayer graphene than those for monolayer graphene, and error margins for three- and four-layer graphene did not allow us to draw a conclusion on the average contact angle value (see Figure S3 in the Supporting Information). Importantly, in all cases graphene showed contact angles different from the contact angle of freshly exfoliated (to avoid airborne hydrocarbons contamination) graphite measured to be 61° ± 3° which is consistent with previously reported values.[8,31–33]

The transparency effect for ice, hydrogel, and copper is even more evident from the surface energy chart (Figure 3b). Surface energy calculations are based on the contact angle measurements with various liquids and are, in that respect, a more comprehensive characteristic of the interactions than a contact angle measurement. Notably, the total surface energy of graphene supported by a substrate is different from the total surface energy of graphite (52 ± 2 mJ m^{-2}) for all tested substrates and equals the surface energy of the bare substrate itself with the only exception of PDMS, as shown in Figure 3b (≈60 mJ m^{-2} for ice, ≈64 mJ m^{-2} for hydrogel, and ≈43 mJ m^{-2} for copper). Thus, although graphene is often considered as a graphite-like material and expected to have graphite-like wetting behavior and surface energy,[5,7,8] clearly, its surface energy and wetting properties are governed by the bulk medium underneath. Furthermore, presence of graphene does not affect the distribution of polar and dispersive forces between the molecules of adsorbate and adsorbent for all types of substrates (the case of PDMS will be discussed further below). Noteworthy, surface energies and polar and dispersive components of the surface energies of ice, graphene-on-ice, hydrogel, and graphene-on hydrogel are all very close to those of pure water, which indicates that ice and hydrogels are suitable as water models for probing wetting properties.

As opposed to graphene-on-ice, graphene-on-hydrogel or graphene-on-copper, graphene transferred onto a Si/SiO_2 wafer or onto a PDMS slab showed significantly different wetting properties than the substrate underneath it (Figure 3a; Figure S4 in the Supporting Information). Moreover, measurements for graphene on SiO_2/Si (but not for bare SiO_2/Si wafers, which were reproducible) were highly irreproducible with all tested liquids with WCA varying from 40° to 90° (Figure S4 in the Supporting Information) and were therefore not included in the present analysis. This can be attributed to the different graphene-substrate adhesion forces that result from sample to sample variation occurring during the transfer process. Although electronic properties of graphene on Si/SiO_2 are well defined in literature, it seems that contamination and even subtle alterations of adhesion forces, that have no effect on the electronic properties, can crucially affect the wetting properties of graphene.

Transfer of graphene to PDMS is more straightforward and, importantly, does not involve coverage of graphene with another polymer than PDMS, permitting reproducible CA measurements (see Methods in the Supporting Information for more details on the transfer).

After transfer of graphene onto PDMS the WCA increased from 33° ± 5° to 91° ± 1° (see Figure 3a) and the total surface energy decreased from 60 ± 1 to 34 ± 1 mJ m^{-2} (Figure 3b). The polar component dropped drastically from 34 ± 1 to 2 ± 1 mJ m^{-2}, whereas the dispersive component

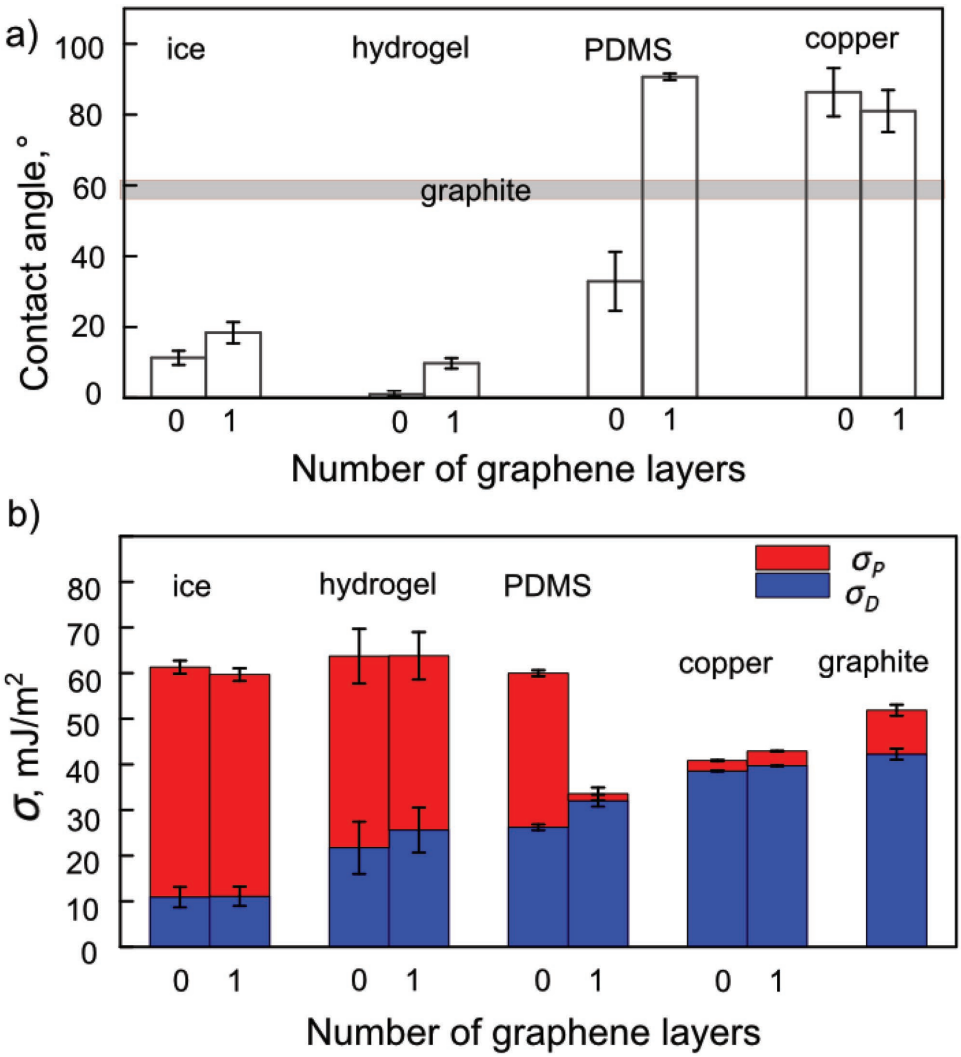

Figure 3. a) Water contact angle of graphene deposited on ice (–20 °C), hydrogel (19.5 °C), PDMS (19.5 °C), and copper (19.5 °C) versus WCA of pristine ice, hydrogel, PDMS, and copper. b) Polar and dispersive components of the surface energy of graphene deposited on ice, hydrogel, PDMS, and copper versus pristine ice, hydrogel, PDMS, and copper. The polar and dispersive components of the surface energy were calculated according the Owens–Wendt theory.

remained almost unchanged at 26 ± 1 mJ m^{-2}. Given the full transparency of graphene to both types of interactions demonstrated above for "well-conforming" substrates, the selective screening of the polar interactions therefore originates from the mismatch in conformation between the surface of graphene and PDMS caused by the transfer process. The lack of conformity between a substrate and graphene transferred on top of it has been independently proven by the atomic force microscopy (AFM) analysis of the surface morphology of PDMS with and without graphene (Figure S5 in the Supporting Information). Graphene transferred to PDMS rather represents the roughness pattern of copper than of PDMS which results in conformational mismatch and breakdown of the wetting transparency of graphene (Figure S5 in the Supporting Information). Polar interactions are short-range and, therefore, evanesce upon increasing the adsorbate–adsorbent distance, whereas long-range dispersion interactions can still be fully transmitted.[34–37] This implies that the observed polar component of 2 ± 1 mJ m^{-2} can be attributed to the inherent polar component of graphene.

Noteworthy, to exclude the influence of adsorbed contaminants from air,[8] samples of graphene on copper and SiO_2/Si were annealed before the measurements (see the Supporting information for more details).

The mechanical fragility of a single layer of graphene floating on the surface of water has prevented so far to probe the surface hydrophilicity by means of contact angle measurements. On water–ice or hydrogels contact angle measurements show that graphene is hydrophilic and transparent to water–water interactions. Importantly, we demonstrated that the interface between the graphene layer and underlying substrate plays an important role: graphene transmits polar and dispersive interactions if the graphene–substrate interface is clean and not corrugated, otherwise polar interactions are screened while dispersive interactions are transmitted. In applications where graphene is suspended between two liquids, these results now shed light and propose

a radically different understanding of the wetting properties of graphene and will have prompt implications in understanding how hydrophobic and hydrophilic molecules interact with the surface of a 2D material subjected to full wetting transparency. We believe that our work will also inspire several research communities to (re)consider how hydrophilicity and hydrophobicity of 2D materials and molecules are defined.

Supporting Information

Supporting Information is available from the Wiley Online Library or from the author.

Acknowledgements

L.A.B. and P.M.G.v.D. contributed equally to this work. This research was supported by the European Research Council under the European Union's Seventh Framework Programme (FP/2007-2013)/ERC Grant Agreement no. 335879 project acronym "Biographene" and the Netherlands Organization for Scientific Research (NWO-VIDI 723.013.007). The authors thank Edgar Blokhuis and Alexander Kros for helpful discussions.

Conflict of Interest

The authors declare no conflict of interest.

Keywords

dispersive interactions, graphene, hydrophilicity, polar interactions, wetting transparency

Received: June 12, 2017
Revised: October 5, 2017
Published online: December 20, 2017

[1] J. Driskill, D. Vanzo, D. Bratko, A. Luzar, *J. Chem. Phys.* **2014**, *141*, 18C517.
[2] J. Rafiee, X. Mi, H. Gullapalli, A. V. Thomas, F. Yavari, Y. Shi, P. M. Ajayan, N. a. Koratkar, *Nat. Mater.* **2012**, *11*, 217.
[3] C.-J. Shih, Q. H. Wang, S. Lin, K.-C. Park, Z. Jin, M. S. Strano, D. Blankschtein, *Phys. Rev. Lett.* **2012**, *109*, 176101.
[4] F. Taherian, V. Marcon, N. F. A. Van Der Vegt, F. Leroy, *Langmuir* **2013**, *29*, 1457.
[5] Y. J. Shin, Y. Wang, H. Huang, G. Kalon, A. T. S. Wee, Z. Shen, C. S. Bhatia, H. Yang, *Langmuir* **2010**, *26*, 3798.
[6] R. Raj, S. C. Maroo, E. N. Wang, *Nano Lett.* **2013**, *13*, 1509.
[7] S. Wang, Y. Zhang, N. Abidi, L. Cabrales, *Langmuir* **2009**, *25*, 11078.
[8] Z. Li, Y. Wang, A. Kozbial, G. Shenoy, F. Zhou, R. Mcginley, P. Ireland, B. Morganstein, A. Kunkel, S. P. Surwade, L. Li, H. Liu, *Nat. Mater.* **2013**, *12*, 925.
[9] N. Ghaderi, M. Peressi, *J. Phys. Chem. C* **2010**, *114*, 21625.
[10] H. Arjmandi-Tash, L. Jiang, G. F. Schneider, *Carbon N. Y.* **2017**, *118*, 556.
[11] L. A. Belyaeva, W. Fu, H. Arjmandi-Tash, G. F. Schneider, *ACS Cent. Sci.* **2016**, *2*, 904.
[12] L. Gao, G.-X. Ni, Y. Liu, B. Liu, A. H. Castro Neto, K. P. Loh, *Nature* **2014**, *505*, 190.
[13] Y. Hwangbo, C.-K. Lee, S.-M. Kim, J.-H. Kim, K.-S. Kim, B. Jang, H.-J. Lee, S.-K. Lee, S.-S. Kim, J.-H. Ahn, S.-M. Lee, *Sci. Rep.* **2014**, *4*, 4439.
[14] H. W. C. Postma, *Nano Lett.* **2010**, *10*, 420.
[15] H. Arjmandi-Tash, L. a. Belyaeva, G. F. Schneider, *Chem. Soc. Rev.* **2016**, *45*, 476.
[16] D. Cohen-Tanugi, J. C. Grossman, *Nano Lett.* **2012**, *12*, 3602.
[17] M. Faraday, *The Athenaeum* **1850**, *1181*, 283.
[18] M. Elbaum, S. G. Lipson, J. G. Dash, *J. Cryst. Growth* **1993**, *129*, 491.
[19] T. Kuroda, R. Lacmann, *J. Cryst. Growth* **1982**, *56*, 189.
[20] H. H. Jellinek, *J. Colloid Sci.* **1959**, *14*, 268.
[21] H. Asakawa, G. Sazaki, K. Nagashima, S. Nakatsubo, Y. Furukawa, *Proc. Natl. Acad. Sci. USA* **2016**, *113*, 1749.
[22] C. J. Van Oss, M. J. Roberts, R. J. Good, M. K. Chaudhury, *Colloids Surf.* **1987**, *23*, 369.
[23] C. J. Van Oss, L. Ju, M. K. Chaudhury, R. J. Good, *J. Colloids Interface Sci.* **1989**, *128*, 313.
[24] D. Zhang, Z. Jin, J. Shi, X. Wang, S. Peng, S. Wang, *Chem. Commun.* **2015**, *51*, 2987.
[25] A. V. Kiselev, *Discuss. Faraday Soc.* **1965**, *40*, 205.
[26] D. K. Owens, R. C. Wendt, *J. Appl. Polym. Sci.* **1969**, *13*, 1741.
[27] F. M. Fowkes, *Ind. Eng. Chem.* **1964**, *56*, 40.
[28] T. Yoon, W. C. Shin, T. Y. Kim, J. H. Mun, T. S. Kim, B. J. Cho, *Nano Lett.* **2012**, *12*, 1448.
[29] S. Deng, V. Berry, *Mater. Today* **2016**, *19*, 197.
[30] X. Tang, S. Xu, J. Zhang, X. Wang, *ACS Appl. Mater. Interfaces* **2014**, *6*, 2809.
[31] M. E. Tadros, P. Hu, A. W. Adamson, *J. Colloid Interface Sci.* **1979**, *72*, 515.
[32] A. Kozbial, C. Trouba, H. Liu, L. Li, *Langmuir* **2017**, *33*, 959.
[33] T. Ondarçuhu, V. Thomas, M. Nuñez, E. Dujardin, A. Rahman, C. T. Black, A. Checco, *Sci. Rep.* **2016**, *6*, 24237.
[34] A. D. Buckingham, *Discuss. Faraday Soc.* **1965**, *40*, 232.
[35] F. L. Leite, C. C. Bueno, A. L. Da Roz, E. C. Ziemath, O. N. Oliveira, *Int. J. Mol. Sci.* **2012**, *28*, 145706.
[36] H. C. Hamaker, *Physica* **1937**, *4*, 1058.
[37] T. Y. Chang, *Rev. Mod. Phys.* **1967**, *39*, 911.